Timer-Based Distributed Node Selection Scheme Exploiting Power Control and Capture

Vikas Kumar Dewangan and Neelesh B. Mehta, *Senior Member, IEEE*

***Abstract*—Opportunistic selection in multi-node wireless systems improves system performance by selecting the "best" node and by using it for data transmission. In these systems, each node has a real-valued local metric, which is a measure of its ability to improve system performance. Our goal is to identify the best node, which has the largest metric. We propose, analyze, and optimize a new distributed, yet simple, node selection scheme that combines the timer scheme with power control. In it, each node sets a timer and transmit power level as a function of its metric. The power control is designed such that the best node is captured even if η other nodes simultaneously transmit with it. We develop several structural properties about the optimal metric-to-timer-and-power mapping, which maximizes the probability of selecting the best node. These significantly reduce the computational complexity of finding the optimal mapping and yield valuable insights about it. We show that the proposed scheme is scalable and significantly outperforms the conventional timer scheme. We investigate the effect of η and the number of receive power levels. Furthermore, we find that the practical peak power constraint has a negligible impact on the performance of the scheme.**

***Index Terms*—Selection, capture, power control, medium access control protocols, timer, distributed schemes.**

I. Introduction

OPPORTUNISTIC selection finds applications in many wireless networks. It exploits spatial diversity in relay-aided cooperative communication systems without requiring tight symbol-level synchronization [1], [2]. It increases spectral efficiency of cellular networks [3]. It also increases network lifetime and reduces energy consumption in sensor networks [4]. Implementing several notions of fairness in scheduling can also be posed as an opportunistic selection problem [3], [5].

In all the above examples, selection involves determining the "best" node from the available nodes, which is subsequently used for data transmission. The notion of the best node can be formalized as follows. Each node possesses a real-valued metric, which is a measure of its ability to improve the system performance. The best node is defined as the node with the largest metric. In general, the metric is system-dependent. For example, in a cellular network, selection of a mobile with the highest downlink channel power gain increases the system throughput [3]. Hence, in this example, the metric of a mobile is its downlink channel power gain. The ratio of the requested throughput to the average throughput of a node is its metric in a proportional fair scheduler [3]. In amplify-and-forward relaying, the harmonic mean of the source-to-relay and relay-to-destination channel gains is the metric of a relay [1].

However, since the nodes are geographically separated, no node in the system knows the metric of any node except itself, and, thus, who the best node is. Hence, a selection scheme is required to identify the best node. One simple selection scheme is polling. In this, each node sequentially communicates its metric to a central node, which then identifies the best node. However, with polling, the time required to communicate the metrics to the central node increases linearly with the number of nodes. This overhead adversely affects the overall system performance and makes the system sensitive to time variations in the channel. Therefore, distributed, scalable selection schemes are necessary.

A. Distributed Node Selection Schemes

Two classes of distributed node selection schemes have been proposed in the literature, namely, splitting and timer schemes. In them, the nodes contend among themselves to send their packets to a common node called sink, which simply selects the node whose packet it successfully decodes first.

In the splitting scheme, nodes whose metrics lie between two thresholds transmit in a slot [6], [7]. The thresholds for the next slot are updated based on the outcome of the current slot. The scheme is such that the best node always transmits any time a transmission occurs. It runs until the best node is selected. While the scheme is fast, it requires a slot-by-slot broadcast of the outcome by the sink.

A timer scheme, on the other hand, runs for a fixed pre-allocated selection duration $T_{\max}$, and does not require any feedback from the sink while it is running [1], [8], [9]. In it, a node i sets its timer based on its metric μ_i. It transmits a timer packet containing its identity and, if needed by the system, its metric to the sink when its timer expires [1], [10]. The metric-to-timer mapping is monotone non-increasing, which ensures that the best node transmits first. However, a collision occurs if a node transmits its packet within a time interval Δ_v after the best node's transmission [8], [11], [12]. The time interval Δ_v is known as the vulnerability window and is determined by the physical layer capabilities of the system. For example, it accounts for propagation delays, time synchronization errors between nodes, and switching times. In the absence of carrier sensing capability in the nodes, it also accounts for the packet

Manuscript received April 8, 2014; revised August 25, 2014; accepted October 22, 2014. Date of publication November 4, 2014; date of current version March 6, 2015. The work of N. B. Mehta was supported in part by the India–U.K. Advanced Technology Center (IU-ATC). The associate editor coordinating the review of this paper and approving it for publication was S. Jin.

The authors are with the Department of Electrical Communication Engineering, Indian Institute of Science (IISc), Bangalore 560012, India (e-mail: dewangan.vikaskumar@gmail.com; nbmehta@ece.iisc.ernet.in).

Digital Object Identifier 10.1109/TWC.2014.2367018

duration. We refer the reader to [8] for an example that gives numerical values for Δ_v based on the IEEE 802.11 physical layer.

Thus, unlike splitting, the timer scheme is simpler and requires minimal feedback. However, it can fail to select the best node for some realizations of the metrics. Consequently, the probability that the best node gets selected within $T_{\max}$, which we henceforth refer to as the *success probability*, is an important performance measure for the timer scheme [8], [11].

B. Contributions

In this paper, we develop a powerful new approach to improve the timer scheme that is based on transmit power control. In it, the metric of a node determines not only its timer, but also its transmit power and, thus, receive power. Power control facilitates the exploitation of the capture effect, in which the timer packet of a node can be decoded even in the presence of simultaneous transmissions by other nodes so long as its signal-to-interference-plus-noise-ratio (SINR) at the sink exceeds a decoding threshold γ [13]–[15]. Without power control, such simultaneous transmissions would have resulted in a collision.

Since success or failure depends on the receive power at the sink, we shall specify the scheme in terms of the target receive power. This can then be translated into transmit power by scaling the target receive power with the inverse of channel power gain between the node and the sink. The target receive power is drawn from a set of L power levels $Q_L = \{q_1, q_2, \ldots, q_L\}$, with $q_1 < q_2 < \cdots < q_L$. These levels are chosen such that they facilitate capture, i.e., the best node with a given target receive power will get decoded even when up to η nodes with lower target receive powers transmit within a duration Δ_v of the transmission by the best node. We shall refer to η as the *interference sustainability factor*. Formally, in the proposed scheme, a node, based on its metric, sets both its timer and target receive power level using a metric-to-timer-and-power mapping $g : \mathcal{U} \to \mathcal{T} \times Q_L$, where $\mathcal{U}$ is the range of values a metric can take and $\mathcal{T} = [0, T_{\max})$.

Our specific contributions are as follows. We first define an *admissible* metric-to-timer-and-power mapping. It generalizes the conditions imposed on conventional metric-to-timer mappings without power control [1], [8], [11] and makes the timer scheme simple and appealing. We then characterize the structure of an optimal mapping that maximizes the success probability. We show that in an optimal mapping, a node can choose its timer from a set of discrete timer values. We then present a general recursion for the optimal success probability that holds for any η and L. These results together enable an optimal mapping to be computed efficiently.

Our next contribution is a closed-form characterization of an optimal mapping for $L = 2$ with $\eta = 1$, and of near-optimal mappings that maximize a tight lower bound on the success probability for $L = 2$ with $\eta = 2$ and $L = 3$ with $\eta = 1$. We show that the recursions simplify considerably in the asymptotic regime of a large number of nodes. Our numerical results show that the above cases deliver most of the gains achievable by power control, and that these gains are significant over the benchmark conventional timer scheme.

C. Connections and Differences From Related Works

In the following, we summarize the connections and differences with several related works on multiple-access (MAC) protocols, selection schemes, and power control. Power control has been used to improve the performance of MAC protocols [3], [16], [17]. While the goal of a MAC protocol is to maximize the system throughput or to minimize latency, a selection scheme focuses on selecting the best node. Power control has also been used to speed up the splitting scheme [15], [18]. However, our application of power control to the timer scheme is novel when compared to [1], [8], [11], [12], [19], [20], and requires a different approach.

We note that the optimality of the discrete timer mapping was shown in [8], [11] without power control. In this paper, we show that this result holds even with power control, which is a more general result. It requires a more elaborate proof than in [8], [11], which clearly brings out how capture improves the success probability. This is a stepping stone to our main contributions, which lie in efficiently computing the optimal metric-to-timer-and-power mapping using new recursions. As we shall see, the exploitation of power control involves optimization over many more dimensions.

The performance measure we focus on is different from measures such as symbol error rate, outage probability, diversity order, and throughput, which have been studied, for example, in [1], [21], [22]. This is because these papers evaluate the performance of the data transmission phase in which the selected node is used for data transmission. In these papers, it is often assumed that the best node has already been selected. We also note that the usage of the term 'distributed selection' in these papers refers to selection combining, i.e., data transmission by the selected relay, and is not to be confused with the distributed selection schemes investigated in this paper and in [1], [6]–[8], [11]. While the timer scheme is considered in [9], it is assumed in its diversity multiplexing trade-off analysis that the best node is always selected, which makes the design of the timer mapping irrelevant.

The paper is organized as follows. Section II presents the system model. In Section III, we elucidate the structure of an optimal metric-to-timer-and-power mapping. In Section IV, we characterize the optimal mappings for two and three power levels. Numerical results and benchmarking are presented in the Section V, and our conclusions follow in Section VI.

II. System Model

We consider a system with $K \geq 2$ nodes since no selection is required when there is only one node. Each node i has a real-valued metric μ_i, which only it knows. The metrics are assumed to be independent and identically distributed (i.i.d.) random variables (RVs), and are uniformly distributed in [0,1) [8], [23], [24]. The independence assumption is justified because the metrics typically depend on the channel gains and the nodes are spatially several wavelengths apart. The assumption about statistically identical metrics, which is common in the aforementioned selection literature, makes the optimization tractable.[1] Assuming a uniform distribution for the metrics does not incur any loss in generality because if μ_i has a continuous cumulative distribution function (CDF) C, then $\kappa_i = C(\mu_i)$ can be alternatively defined as the new metric. It is uniformly distributed between [0,1) and preserves order [25]. The CDF changes at a rate that is several orders of magnitude slower than the metrics, and, thus, can be estimated with sufficient accuracy [26]. Consequently, its knowledge has been assumed in [8], [11], [23], [24] as well.

Following order statistics notation, $[i]$ denotes the node with the i^{th} largest metric $\mu_{[i]}$. Therefore, $\mu_{[1]} \geq \mu_{[2]} \geq \cdots \geq \mu_{[N]}$ and node $[1]$ is the best node. During the selection process, which lasts for a duration $T_{\max}$, the sink receives the transmissions of the nodes. Node $[1]$ gets selected by the sink only if its SINR at the sink, which is denoted by $\text{SINR}_{[1]}$, is greater than or equal to a threshold γ.[2] When M nodes $[1], [2], \ldots, [M]$ transmit within an interval Δ_v, $\text{SINR}_{[1]}$ equals

$$\text{SINR}_{[1]} = \frac{\varphi_{[1]}}{\sum_{j=2}^{M} \varphi_{[j]} + \sigma^2} \tag{1}$$

where $\varphi_{[i]}$ is the target receive power of node $[i]$ and σ^2 is the noise power at the receiver. In this setting, a collision is said to occur if $\text{SINR}_{[1]} < \gamma$ and the scheme is said to fail.[3]

A node $[i]$ based on its metric $\mu_{[i]}$ sets its timer value $T_{[i]} \in \mathcal{T}$ and its target receive power $\varphi_{[i]} \in \mathcal{Q}_L$. As mentioned, the target receive powers are set such that $\text{SINR}_{[1]}$ exceeds γ even if as many as η other nodes with target receive powers less than $\varphi_{[1]}$ transmit in the time interval $[T_{[1]}, T_{[1]} + \Delta_v)$. Furthermore, the lowest power level q_1 is set equal to or greater than $\gamma\sigma^2$ so that if the best node transmits with target receive power q_1 and no other node transmits in $[T_{[1]}, T_{[1]} + \Delta_v)$, then its signal-to-noise-ratio (SNR) exceeds γ and it, thus, gets decoded. Therefore,

$$q_1 \geq \gamma\sigma^2 \text{ and } q_j \geq \gamma(\eta q_{j-1} + \sigma^2), \text{ for } 2 \leq j \leq L.$$

We choose the following lowest possible values of the target power levels that satisfy the above constraints as this leads to the lowest transmit and receive power dynamic ranges:

$$q_1 = \gamma\sigma^2 \text{ and } q_j = \gamma(\eta q_{j-1} + \sigma^2), \text{ for } 2 \leq j \leq L. \tag{2}$$

Transmit Power Setting: To achieve a target receive power q_j at the sink, a node i sets its transmit power equal to q_j/h_i, where h_i is the channel power gain from node i to the sink. With this transmit power, the receive power is $h_i(q_j/h_i) = q_j$. The knowledge of h_i can be acquired either by exploiting reciprocity or by periodic feedback from the sink.

[1] We note that the proposed scheme works even with non-i.i.d. metrics, except that its optimality is no longer guaranteed.

[2] The threshold γ depends on the modulation and coding scheme and is of the order of 8 to 10 dB. In our model, at most one node gets selected, unlike code division multiple access systems.

[3] A more refined model for the SINR would also factor in the extent of overlap between the packets of different nodes [27]. However, this makes the problem intractable and is beyond the scope of this paper. We note that the conventional collision model, which has driven the design of most of the selection schemes thus far, also does not take such overlap into account.

Notation: We define two projection functions Ξ_T and Ξ_P on a tuple (x,y) as follows:

$$\Xi_T(x,y) = x \text{ and } \Xi_P(x,y) = y. \tag{3}$$

The probability of an event $\mathcal{E}$ is denoted by $\Pr(\mathcal{E})$. Similarly, the conditional probability of $\mathcal{E}$ given $\mathcal{F}$ is denoted by $\Pr(\mathcal{E}|\mathcal{F})$. The multinomial term $\binom{K}{i_1, i_2, \ldots, i_n}$ stands for $K!/(i_1! i_2! \ldots i_n! (K - i_1 - i_2 - \ldots - i_n)!)$. And, $\lfloor \cdot \rfloor$ denotes the floor function.

III. Optimal Timer Scheme With Power Control

To incorporate power control, we first generalize the monotonically non-increasing property required of timer mappings in [1], [8]. This property has made timer schemes popular because it ensures that the first timer to expire is from the best node.

Definition: A metric-to-timer-and-power mapping $g(\mu)$ is said to be *admissible* if the transmission by the best node happens no later than any other node, and if a node gets selected then it is the best node.

Notice the additional constraint about which node gets selected. Since the mapping $g(.)$ is from $\mathcal{U}$ to $\mathcal{T} \times \mathcal{Q}_L$, it follows from the definition above that $\Xi_T(g(\mu_{[k]})) \leq \Xi_T(g(\mu_{[l]}))$, for all $1 \leq k, l \leq K$ and $k < l$. Our goal is to find an optimal mapping in the space of all admissible mappings. We now show an important property of an optimal mapping. Let $\mathcal{V}_D$ denote the special set of all admissible mappings $\mathcal{U} \to \mathcal{T}_N \times \mathcal{Q}_L$, where $\mathcal{U} = [0,1)$, $\mathcal{T}_N = \{0, \Delta_v, \ldots, N\Delta_v\}$, and $N = \lfloor T_{\max}/\Delta_v \rfloor$, i.e., the timer expires only at $0, \Delta_v, \ldots, N\Delta_v$.

Result 1: An optimal metric-to-timer-and-power mapping lies in the smaller space of admissible mappings $\mathcal{V}_D$.

Proof: A constructive proof is given in Appendix A. ■

From the definition of $\mathcal{V}_D$, for each mapping in $\mathcal{V}_D$, there exists an interval length vector (ILV) $\boldsymbol{\alpha}_N = (\alpha_N[0], \alpha_N[1], \ldots, \alpha_N[N])$, where $\alpha_N[i] \geq 0$, for $0 \leq i \leq N$, and $0 \leq \sum_{i=0}^{N} \alpha_N[0] \leq 1$, such that if a node's metric lies in the interval $\mathcal{A}_N(0) \stackrel{\Delta}{=} [1 - \alpha_N[0], 1)$, then the node transmits at time instant 0, if it lies in the interval $\mathcal{A}_N(1) \stackrel{\Delta}{=} [1 - \alpha_N[0] - \alpha_N[1], 1 - \alpha_N[0])$, then it transmits at time instant Δ_v, and so on. In general, if a node's metric lies in the interval $\mathcal{A}_N(j) \stackrel{\Delta}{=} [1 - \sum_{i=0}^{j} \alpha_N[i], 1 - \sum_{i=0}^{j-1} \alpha_N[i])$, which is of length $\alpha_N[j]$, then the node sets its timer value to $j\Delta$. Henceforth, we say that a node lies in an interval if its metric lies in the interval. The following result elucidates the structure of any mapping in $\mathcal{V}_D$.

Result 2: Every mapping in $\mathcal{V}_D$ must satisfy the following property: if nodes $[i]$ and $[k]$ have the same timer value, i.e., if $T_{[i]} = T_{[k]}$ and $i < k$, then $\varphi_{[i]} \geq \varphi_{[k]}$.

Proof: Let there be a mapping in $\mathcal{V}_D$ that does not satisfy the above property. Therefore, for some j, there exist at least two non-overlapping subintervals (z_1, z_2) and (z_3, z_4) in the interval $\mathcal{A}_N(j)$, where $z_1 < z_2 < z_3 < z_4$, such that the target receive power assigned to a node that lies in (z_1, z_2) is greater than that assigned to a node that lies in (z_3, z_4). Now, consider a realization of metrics in which $\mu_{[2]} \in (z_1, z_2)$, $\mu_{[1]} \in (z_3, z_4)$, and $\mu_{[3]} \notin \mathcal{A}_N[j]$. This occurs with non-zero probability. In this realization, node [2] will get selected instead of node [1] because

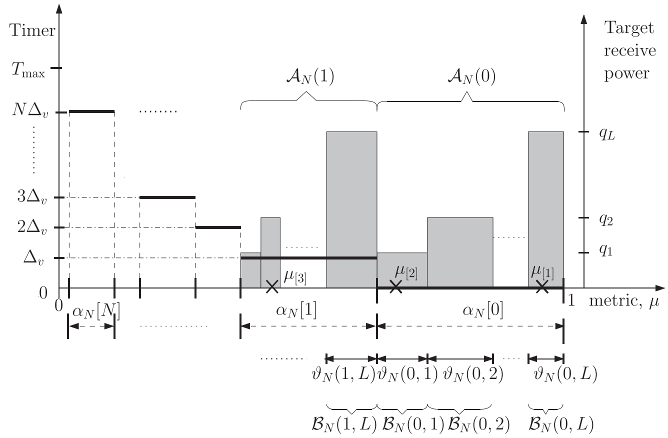

Fig. 1. Illustration of metric-to-timer-and-power mapping and how different metrics lead to different timers and target receive powers. The shaded vertical bars represent target receive power.

$\varphi_{[2]} > \varphi_{[1]}$. Hence, the mapping is inadmissible, and it cannot be in $\mathcal{V}_D$. ■

Result 2 implies that in an admissible mapping, a node with a higher metric will never transmit with a target receive power that is less than that of the other nodes that simultaneously transmit with it. It ensures selection of the best node in case a node gets selected. It also implies that each interval $\mathcal{A}_N(i)$ can be partitioned into L subintervals denoted by the set $\boldsymbol{B}_N(i) = \{\mathcal{B}_N(i,1), \mathcal{B}_N(i,2), \ldots, \mathcal{B}_N(i,L)\}$ such that if a node lies in $\mathcal{B}_N(i,j)$ then it sets its timer value to $i\Delta_v$ and its target receive power to q_j. Let the length of $\mathcal{B}_N(i,j)$ be denoted by $\vartheta_N(i,j)$. Then, $\sum_{j=1}^{L} \vartheta_N(i,j) = \alpha_N[i]$.

Let Ω_i be the fraction of N nodes that transmit at time $i\Delta_v$. Let $f_N(i,l)$ be the fraction of Ω_i nodes that transmit with target receive power q_l. Clearly, $f_N(i,l) = \vartheta_N(i,l)/\alpha_N[i] \geq 0$ and $\sum_{l=1}^{L} f_N(i,l) = 1$, $\forall i$. We define the *power distribution* matrix (PDM) $\boldsymbol{F}_N$ as

$$\boldsymbol{F}_N \triangleq \begin{bmatrix} f_N(0,1) & f_N(0,2) & \ldots & f_N(0,L) \\ f_N(1,1) & f_N(1,2) & \ldots & f_N(1,L) \\ & \vdots & & \\ f_N(N,1) & f_N(N,2) & \ldots & f_N(N,L) \end{bmatrix}. \quad (4)$$

The $(i+1)^{\text{th}}$ row of $\boldsymbol{F}_N$ is denoted by $\boldsymbol{F}_N(i,:)$.

The above concepts are illustrated in Fig. 1, which plots the target receive power level and the timer value of the node as a function of the node metric for $K = 3$ nodes. In the figure, we have $\mu_{[1]} \in \mathcal{B}_N(0,L) \subset \mathcal{A}_N(0)$, $\mu_{[2]} \in \mathcal{B}_N(0,1) \subset \mathcal{A}_N(0)$, and $\mu_{[3]} \in \mathcal{B}_N(1,2) \subset \mathcal{A}_N(1)$. Hence, node [1] sets its timer and target receive power to 0 and q_L, respectively, node [2] sets its timer and target receive power to 0 and q_1, respectively, and node [3] to Δ_v and q_2, respectively. As a result, node [1] gets selected.

From Results 1 and 2, it follows that for a given N and L, the success probability $P_N(\boldsymbol{\alpha}_N, \boldsymbol{F}_N)$ depends on $\boldsymbol{\alpha}_N$ and $\boldsymbol{F}_N$. We shall, therefore, use the tuple $[\boldsymbol{\alpha}_N, \boldsymbol{F}_N]$ to refer to the mapping itself. Hence, the total number of variables to be optimized for the timer scheme with power control is $(N+1)L$. This is a factor of L larger than the number of variables to be optimized without power control in [8]. Let the optimal success probability be denoted by P_N^*. The ILV and the PDM that achieve P_N^* will be referred to as the optimal ILV $\boldsymbol{\alpha}_N^*$ and the optimal PDM $\boldsymbol{F}_N^*$, respectively.

IV. Structure of Optimal Mapping and Analysis

In this section, we first present a general recursion for determining P_N^*, $\boldsymbol{\alpha}_N^*$, and $\boldsymbol{F}_N^*$ in terms of those for $N-1$. We then show that it simplifies for the following scenarios: i) $L = 2$ with $\eta = 1$, ii) $L = 2$ with $\eta = 2$, and iii) $L = 3$ with $\eta = 1$. These give insights about the role of η and L in determining the optimal mapping and its success probability. The analysis for larger values of η and L is more involved, yields limited additional insights, and, as we shall see, limited gains over the above reference scenarios.

A. General Recursion

From the law of total probability, the probability of success $P_N(\boldsymbol{\alpha}_N, \boldsymbol{F}_N)$ is given by

$$\begin{aligned} P_N(\boldsymbol{\alpha}_N, \boldsymbol{F}_N) &= \Pr(\mathcal{S}_0) + \Pr\left(\text{Success}|\overline{\mathcal{S}_0}\right)\Pr(\overline{\mathcal{S}_0}), \\ &= \Pr(\mathcal{S}_0) + (1-\alpha_N[0])^K \\ &\quad \times P_{N-1}\left(\boldsymbol{\alpha}'_{N-1}, \boldsymbol{F}'_{N-1}\right), \end{aligned} \quad (5)$$

where $\mathcal{S}_0$ denotes success at $t = 0$ and $\overline{\mathcal{S}_0}$ denotes its complement. The elements of vector $\boldsymbol{\alpha}'_{N-1}$, which is of length N, are given for $\alpha_N[0] \neq 1$ by

$$\alpha'_{N-1}[i] = \frac{\alpha_N[i+1]}{1-\alpha_N[0]}, \quad 0 \leq i \leq N-1, \quad (6)$$

and the elements of matrix $\boldsymbol{F}'_{N-1}$, of size $N \times L$, by

$$f'_{N-1}(i,l) = f_N(i+1,l), \quad \text{for } 0 \leq i \leq N-1 \text{ and } 1 \leq l \leq L. \quad (7)$$

Equation (5) follows because a success at a later time instant can occur only when there is no transmission $t = 0$, which occurs only if no node lies in the interval $[1-\alpha_N[0], 1)$. This happens with probability $(1-\alpha_N[0])^K$. Given that no node transmits at $t = 0$, the metrics of the K nodes are i.i.d. and uniformly distributed in $[0, 1-\alpha_N[0])$, and the total time available for selection decreases to $T_{\max} - \Delta_v$, for which the success probability is $P_{N-1}(\boldsymbol{\alpha}'_{N-1}, \boldsymbol{F}'_{N-1})$.

By definition, $P_{N-1}^* \geq P_{N-1}(\boldsymbol{\alpha}'_{N-1}, \boldsymbol{F}'_{N-1})$. Hence, $P_N(\boldsymbol{\alpha}_N, \boldsymbol{F}_N)$ in (5) satisfies the bound

$$P_N(\boldsymbol{\alpha}_N, \boldsymbol{F}_N) \leq \Pr(\mathcal{S}_0) + (1-\alpha_N[0])^K P_{N-1}^*. \quad (8)$$

Further, this upper bound is achieved by setting $\alpha_N[i+1] = \alpha_{N-1}^*[i](1-\alpha_N[0])$, for $0 \leq i \leq N-1$, and $f_N(i+1,j) = f_{N-1}^*(i,j)$, for $0 \leq i \leq N-1$ and $1 \leq j \leq L$. Therefore,

$$\{\boldsymbol{\alpha}_N^*, \boldsymbol{F}_N^*\} = \underset{\substack{\alpha_N[0], \boldsymbol{F}_N[0,:] \\ \sum_{j=1}^{L} f_N(0,j)=1}}{\arg\max} \left\{\Pr(\mathcal{S}_0) + (1-\alpha_N[0])^K P_{N-1}^*\right\}. \quad (9)$$

The probability of success at $t = 0$ depends only on the number of nodes whose metrics lie in the intervals $\mathcal{B}_N(0,1)$, $\mathcal{B}_N(0,2),\ldots,\mathcal{B}_N(0,L)$. It is given by

$$\Pr(\mathcal{S}_0) = \sum_{\boldsymbol{u}\in\Lambda} \binom{K}{u_1,u_2,\ldots,u_L} \left[\prod_{j=1}^{L} (\alpha_N[0] f_N(0,j))^{u_j}\right] \times (1-\alpha_N[0])^{K-\sum_{j=1}^{L} u_j}, \quad (10)$$

where Λ is the set of all L-tuples $\boldsymbol{u} = (u_1,u_2,\ldots,u_L)$, such that if $u_1,u_2,\ldots,u_L$ nodes transmit with target receive power $q_1,q_2,\ldots,q_L$, respectively, at $t = 0$ then a success occurs at $t = 0$. Mathematically, Λ is the set of all L-tuples $\boldsymbol{u} = (u_1,u_2,\ldots,u_L)$, such that $\sum_{j=1}^{L} u_j \le K$, $u_j \in \{0\}\cup\mathbb{Z}^+$, for $1 \le j \le L$, and there exists a j_0 such that $u_{j_0} = 1$ and $u_{j_0+1} = u_{j_0+2} = \cdots = u_L = 0$, and $q_{j_0}/(\sum_{j=1}^{j_0-1} q_j u_j + \sigma^2) \ge \gamma$. This means that the best node has target receive power q_{j_0}, the other nodes that transmit at $t = 0$ have lower target receive powers, and $\mathrm{SINR}_{[1]} \ge \gamma$. Hence, P_N^* is given by

$$P_N^* = \sum_{\boldsymbol{u}\in\Lambda} \binom{K}{u_1,u_2,\ldots,u_L} \left[\prod_{j=1}^{L} (\alpha_N^*[0] f_N^*(0,j))^{u_j}\right] \times (1-\alpha_N^*[0])^{K-\sum_{j=1}^{L} u_j} + (1-\alpha_N^*[0])^K P_{N-1}^*, \quad (11)$$

where $P_{-1}^* = 0$.

In general, the recursion in (11) is solved numerically. It reduces the search complexity to L variables because, given P_{N-1}^*, only the L variables $\alpha_N[0]$, $f_N(0,1)$, $f_N(0,2),\ldots,f_N(0,L-1)$ need to be optimized. We now state a useful property of the optimal mapping.

Result 3: $\alpha_N^*[0] \in (0,1)$. Further, when $L \ge 2$, no element of $\boldsymbol{F}_N^*$ is equal to one.

Proof: The proof is given in Appendix B. ■

B. Two Target Receive Power Levels ($L = 2$) *With* $\eta = 1$

Result 4: For $L = 2$ with $\eta = 1$, the optimal success probability is given by

$$P_N^* = (1-\alpha_N^*[0])^K P_{N-1}^* + K\alpha_N^*[0](1-\alpha_N^*[0])^{K-1} + \binom{K}{1,1}\frac{(\alpha_N^*[0])^2(1-\alpha_N^*[0])^{K-2}}{4}. \quad (12)$$

The elements of $\boldsymbol{\alpha}_N^*$ and $\boldsymbol{F}_N^*$ are given by the recursion

$$\alpha_N^*[0] = \begin{cases} \frac{1}{4}, & K=5, N=0,\\ \frac{\upsilon_1(K,P_{N-1}^*)+\sqrt{\upsilon_2(K,P_{N-1}^*)}}{\upsilon_3(K,P_{N-1}^*)}, & \text{otherwise,}\end{cases} \quad (13)$$

$$\alpha_N^*[i] = \alpha_{N-1}^*[i-1](1-\alpha_N^*[0]), \text{ for } 1 \le i \le N, \quad (14)$$

$$\text{and } f_N^*(i,1) = f_N^*(i,2) = \frac{1}{2}, \text{ for } 0 \le i \le N. \quad (15)$$

Here, $\upsilon_1(K,P_{N-1}^*) = -(K+3-4P_{N-1}^*)$, $\upsilon_2(K,P_{N-1}^*) = (5K-9)(K-1) - P_{N-1}^*(4K-8)(K-1)$, and $\upsilon_3(K,P_{N-1}^*) = K(K-5) + 4P_{N-1}^*$.

Proof: The proof is given in Appendix C. ■

Note that unlike (11), now no numerical search is required.

Asymptotic Behavior: To gain more insights, we now study the regime in which $K \to \infty$. In this regime, it can be shown from (13) and (14) that $\alpha_N^*[i] \to 0$. Let $\boldsymbol{\beta}_N^* = \lim_{K\to\infty} K\boldsymbol{\alpha}_N^*$. Further, since $\lim_{K\to\infty}(1-\alpha_N^*[0])^K = (1-\beta_N^*[0]/K)^K = e^{-\beta_N^*[0]}$, (12) simplifies to $P_N^* = e^{-\beta_N^*[0]}(\beta_N^*[0] + (\beta_N^*[0])^2/4 + P_{N-1}^*)$. Taking limits on both sides of (13) and (14), we get

$$\beta_N^*[i] = \begin{cases} -1+\sqrt{5-4P_{N-1}^*}, & i = 0,\\ \beta_{N-1}^*[i-1], & 1 \le i \le N.\end{cases} \quad (16)$$

Substituting $P_{N-1}^* = (5-(\beta_N^*[0]+1)^2)/4$ from (16) in the expression for P_N^* above yields the following simpler and elegant result:

$$P_N^* = e^{-\beta_N^*[0]}\left(1+\frac{\beta_N^*[0]}{2}\right). \quad (17)$$

C. Two Target Receive Power Levels ($L = 2$) *With* $\eta = 2$

For this case, even a closed-form, recursive characterization along the lines of Result 4 is difficult. We, therefore, present a simple recursive, closed-form solution of a lower bound on P_N^*. We shall see in Section V that it is tight.

Result 5: The optimal success probability P_N^* is lower bounded by $\check{P}_N^*$, where

$$\check{P}_N^* = (1-\check{\alpha}_N^*[0])^K \check{P}_{N-1}^* + K\check{\alpha}_N^*[0](1-\check{\alpha}_N^*[0])^{K-1} + \frac{1}{4}\binom{K}{1,1}(\check{\alpha}_N^*[0])^2(1-\check{\alpha}_N^*[0])^{K-2} + \frac{1}{8}\binom{K}{2,1}(\check{\alpha}_N^*[0])^3(1-\check{\alpha}_N^*[0])^{K-3}, \quad (18)$$

and $\check{P}_{-1}^* = 0$. This bound is achieved with ILV $\check{\boldsymbol{\alpha}}_N^*$ and PDM $\check{\boldsymbol{F}}_N^*$, whose elements are given by

$$\check{\alpha}_N^*[0] = \begin{cases} \frac{1}{4}, & K=5, N=0,\\ \frac{\upsilon_1(K,\check{P}_{N-1}^*)+\sqrt{\upsilon_2(K,\check{P}_{N-1}^*)}}{\upsilon_3(K,\check{P}_{N-1}^*)}, & \text{otherwise,}\end{cases} \quad (19)$$

$$\check{\alpha}_N^*[i] = \check{\alpha}_{N-1}^*[i-1](1-\check{\alpha}_N^*[0]), \text{ for } 1 \le i \le N, \quad (20)$$

$$\text{and } \check{f}_N^*(i,1) = \check{f}_N^*(i,2) = \frac{1}{2}, \text{ for } 0 \le i \le N. \quad (21)$$

The functions υ_1, υ_2, and υ_3 are defined in Result 4.

Proof: The proof and the intuition behind the recursion are given in Appendix D. ■

As before, no numerical search is required here, unlike (11). There is one important difference between the recursions in (13) and (19), which is that the success probability expression in (18) is based on $L = 2$ with $\eta = 2$ and not on $L = 2$ with $\eta = 1$. This approach can be further extended to obtain a lower bound for P_N^* for $L = 2$ and any $\eta \geq 3$.

Asymptotic Behavior: Let $\check{\boldsymbol{\beta}}_N^* = \lim_{K\to\infty} K\check{\boldsymbol{\alpha}}_N^*$. As $K \to \infty$, (18) simplifies to $\check{P}_N^* = e^{-\check{\beta}_N^*[0]}(\check{\beta}_N^*[0] + (\check{\beta}_N^*[0])^2/4 + (\check{\beta}_N^*[0])^3/16 + \check{P}_{N-1}^*)$. Taking limits on both sides of (19) and (20), we get

$$\check{\beta}_N^*[i] = \begin{cases} -1 + \sqrt{5 - 4\check{P}_{N-1}^*}, & i = 0, \\ \check{\beta}_{N-1}^*[i-1], & 1 \leq i \leq N. \end{cases} \tag{22}$$

Substituting $\check{P}_{N-1}^* = (5 - (\check{\beta}_N^*[0] + 1)^2)/4$ from (22) in the expression for $\check{P}_N^*$ above, we get

$$\check{P}_N^* = e^{-\check{\beta}_N^*[0]} \left(1 + \frac{\check{\beta}_N^*[0]}{2} + \frac{\left(\check{\beta}_N^*[0]\right)^3}{16} \right). \tag{23}$$

D. Three Target Receive Power Levels ($L = 3$) With $\eta = 1$

This case is even more involved than the above case. Therefore, as before, we present a lower bound, which the numerical results in Section V show is tight.

Result 6: The success probability P_N^* is lower bounded by $\widetilde{P}_N^*$, where

$$\widetilde{P}_N^* = (1 - \widetilde{\alpha}_N^*[0])^K \widetilde{P}_{N-1}^* + K\widetilde{\alpha}_N^*[0] (1 - \widetilde{\alpha}_N^*[0])^{K-1} + \binom{K}{1,1} \frac{(\widetilde{\alpha}_N^*[0])^2 (1 - \widetilde{\alpha}_N^*[0])^{K-2}}{3}, \tag{24}$$

and $\widetilde{P}_{-1}^* = 0$. The elements of the ILV $\widetilde{\boldsymbol{\alpha}}_N^*$ and the PDM $\widetilde{\boldsymbol{F}}_N^*$, which achieve $\widetilde{P}_N^*$, are given by

$$\widetilde{\alpha}_N^*[0] = \begin{cases} \frac{1}{3}, & K = 4, N = 0, \\ \frac{\upsilon_4(K, \widetilde{P}_{N-1}^*) + \sqrt{\upsilon_5(K, \widetilde{P}_{N-1}^*)}}{\upsilon_6(K, \widetilde{P}_{N-1}^*)}, & \text{otherwise}, \end{cases} \tag{25}$$

$$\widetilde{\alpha}_N^*[i] = \widetilde{\alpha}_{N-1}^*[i-1] (1 - \widetilde{\alpha}_N^*[0]), \text{ for } 1 \leq i \leq N, \tag{26}$$

$$\text{and } \widetilde{f}_N^*(i,1) = \widetilde{f}_N^*(i,2) = \widetilde{f}_N^*(i,3) = \frac{1}{3}, \text{ for } 0 \leq i \leq N. \tag{27}$$

Here, $\upsilon_4(K, \widetilde{P}_{N-1}^*) = -(K + 5 - 6\widetilde{P}_{N-1}^*)$, $\upsilon_5(K, \widetilde{P}_{N-1}^*) = (13K - 25)(K-1) - \widetilde{P}_{N-1}^*(12K - 24)(K-1)$, and $\upsilon_6(K, \widetilde{P}_{N-1}^*) = 2(K^2 - 4K + 3\widetilde{P}_{N-1}^*)$.

Proof: The proof is given in Appendix E. ■

Here again no numerical search is required unlike (11).

Asymptotic Behavior: Let $\widetilde{\boldsymbol{\beta}}_N^* = \lim_{K\to\infty} K\widetilde{\boldsymbol{\alpha}}_N^*$. Then, as $K \to \infty$, (24) simplifies to $\widetilde{P}_N^* = e^{-\widetilde{\beta}_N^*[0]}(\widetilde{\beta}_N^*[0] + (\widetilde{\beta}_N^*[0])^2/3 + \widetilde{P}_{N-1}^*)$. Further, from (25) and (26), we get

$$\widetilde{\beta}_N^*[i] = \begin{cases} \frac{-1 + \sqrt{13 - 12\widetilde{P}_{N-1}^*}}{2}, & i = 0, \\ \widetilde{\beta}_{N-1}^*[i-1], & 1 \leq i \leq N. \end{cases} \tag{28}$$

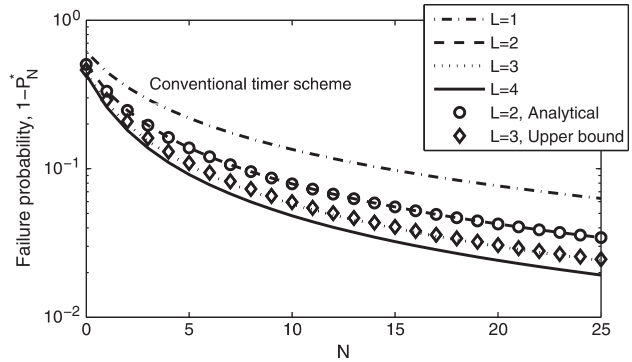

Fig. 2. Failure probability $1 - P_N^*$ for different number of power levels and N ($K = 10$ and $\eta = 1$).

Substituting $\widetilde{P}_{N-1}^* = 1 - (\widetilde{\beta}_N^*[0] + (\widetilde{\beta}_N^*[0])^2)/3$ from (28) in the expression for $\widetilde{P}_N^*$ above yields

$$\widetilde{P}_N^* = e^{-\widetilde{\beta}_N^*[0]} \left(1 + \frac{2\widetilde{\beta}_N^*[0]}{3} \right). \tag{29}$$

Insights From Asymptotic Results: As P_N^*, $\check{P}_N^*$, and $\widetilde{P}_N^*$ are all monotonically increasing functions of N, we see from (16) and (17), (22) and (23), and (28) and (29) that for any N, the optimal success probability for $L = 2$ with $\eta = 1$, $L = 2$ with $\eta = 2$, and $L = 3$ with $\eta = 1$ is never less than $P_0^* = 0.47$, $\check{P}_0^* = 0.50$, and $\widetilde{P}_0^* = 0.51$, respectively, as $K \to \infty$. These show that the scheme is scalable. These values are significantly higher than $P_0^* = 1/e = 0.37$ for $L = 1$ [8]. Further, we can show that $\beta_N^*[i]$ is a monotonically decreasing function of N when $i = 0$ and a monotonically increasing function of i for a given N. Thus, when the time available for selection is less, the scheme is more aggressive in terms of the number of nodes on average that transmit next. The same is observed for $L = 2$ and $\eta = 2$, and $L = 3$ and $\eta = 1$. Furthermore, it can be shown that $P_N^* < \check{P}_N^*$, $\forall N$, which mathematically explains why increasing η improves the success probability.

V. Results

We now evaluate the efficacy of the proposed approach for different system parameter settings. We verify the analytical results with Monte Carlo simulation results, which are generated using 50 000 runs. We also evaluate the tightness of the lower bounds derived in Section IV-C and D. Unless mentioned otherwise, $\gamma = 10$ dB and $\sigma^2 = -110$ dBm.

Fig. 2 plots the performance of the optimal mapping as a function of N, which is equivalent to $T_{\max}$. This is done for $\eta = 1$ for one (no power control) [8], two, three, and four target receive power levels. The latter three cases are obtained by numerically solving (11). To ensure clarity, the failure probability, which is equal to $1 - P_N^*$, is plotted in log scale. We see that the failure probability decreases exponentially as N increases for large enough N. Further, for a given N, having more power levels reduces the failure probability, which demonstrates the advantage of exploiting power control. These are an order of magnitude lower than for the conventional and popular inverse timer mappings [1], [8].

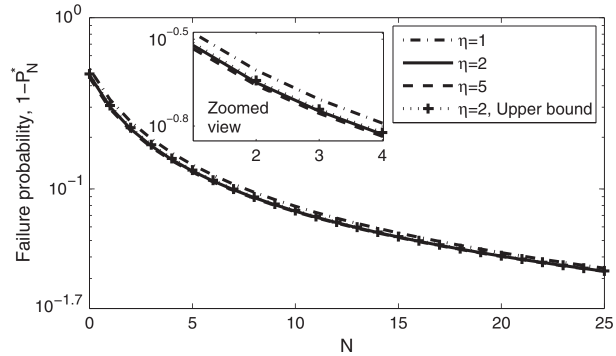

Fig. 3. Zoomed-in view of failure probability $1-P_N^*$ for different interference sustainability factors η as a function of N ($K=10$ and $L=2$).

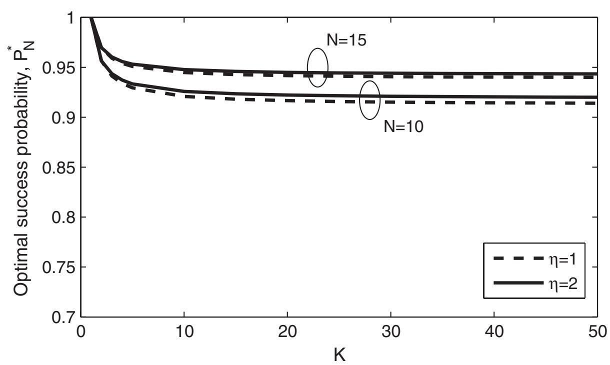

Fig. 4. Scalability evaluation: Zoomed-in view of optimal success probability P_N^* as a function of the number of nodes K for different η ($L=2$).

However, the gains from increasing L diminish once L exceeds 3 due to the law of diminishing returns. The intuition behind it is as follows: when a single node transmits, it is always selected irrespective of L. When two nodes transmit simultaneously at time $i\Delta_v$, a success occurs so long as the target receive power levels of the two nodes are different. (We do not consider events involving transmissions by three or more nodes since these are much less likely.) Given that two nodes transmit at $i\Delta_v$, it can be shown that the success probability is $(1-1/L)/2$. This increases more slowly as L increases and approaches 1/2.

We also plot the analytical result for $L=2$, $\eta=1$, which is given in closed form in Section IV-B. For $L=3$, $\eta=1$ the bound from Section IV-D is also plotted. For failure probability, it is now an upper bound. We see that it is very tight. We also note that the proposed scheme outperforms the centralized polling scheme for $N<K-1$. For example, for $N=6$ and $K=10$ nodes, only 70% of the nodes can sequentially transmit their metrics to the sink. This corresponds to a failure probability of 0.3, which exceeds that of the proposed scheme.

Fig. 3 plots the failure probability in logarithmic scale as a function of N, or, equivalently, the selection duration $T_{\max}$ for $L=2$ with different η. When η increases from 1 to 2, the failure probability visibly decreases. However, beyond $\eta=2$, the decrease is negligible. This justifies our focus on $\eta=1$ and 2. The bound for the failure probability for $\eta=2$ (cf. Section IV-C), is also plotted, and is very tight.

Fig. 4 evaluates the scalability of the proposed scheme. It plots P_N^* as a function of the number of nodes K for two different η and $L=2$. For all η, we see that $P_N^*=1$ when $K=1$, which is intuitive since no collisions occur. Further, P_N^* does not decrease once K exceeds 10, which shows that the proposed scheme is scalable and that the elegant asymptotic regime manifests itself once K exceeds 10.

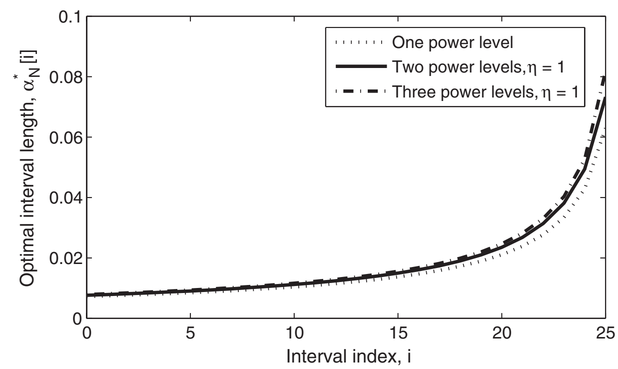

Fig. 5. Effect of number of power levels on optimal interval lengths: $\alpha_N^*[i]$ as a function of i ($N=25$ and $K=10$).

A. Insights About Structure of Optimal Mapping

We now delve deeper into the structure of the optimal timer mappings developed thus far. To this end, we study how the optimal ILV and PDM vary for different L and η.

Fig. 5 plots the optimal interval lengths $\alpha_N^*[i]$ as a function of i for different values of L for $N=25$. First, we observe that for any given L, $\alpha_N^*[i]$ increases with i. This implies that the scheme is initially conservative and makes fewer nodes, on average, to transmit. However, as more idle outcomes occur, i.e., as i increases, $\alpha_N^*[i]$ increases to increase the odds of transmission. Secondly, we see that given i, $\alpha_N^*[i]$ increases as the number of power levels increases. This is because a larger L facilitates capture better; as a result, more nodes can transmit simultaneously. For the same reason, $\alpha_N^*[i]$ is also a monotonically increasing function of η. This is not shown due to space constraints. We note that this behavior does not affect the selection time, which is pre-fixed at $T_{\max}$ since the timers only expire at $i\Delta_v$, for $0\le i\le N$.

Fig. 6 investigates how the optimal fraction of nodes $f_N^*(i,j)$ that transmit with target receive power q_j changes with i for $L=2$ and different η. For $\eta=1$, $f_N^*(i,j)=1/2$, for all i and j. However, for $\eta=2$, we see $f_N^*(i,1)=1-f_N^*(i,2)$ increases as i increases. This behavior becomes more acute when η is increased to 5.

B. Effect of Peak Power Constraint

In the proposed scheme, node i sets its transmit power to q_j/h_i, where h_i is its uplink channel power gain, in order to attain a target receive power $q_j\in Q_L$ at the sink. In practice, this cannot be achieved if q_j/h_i exceeds a peak transmit power P_{peak}, which affects the performance of the scheme. To study the effect of the peak power constraint, we consider the scenario in which the uplink channel power gain is the node's metric and is a unit mean exponential RV. This models Rayleigh fading. Node i now sets its transmit power to $\min\{P_{\text{peak}},q_j/h_i\}$. Further, it

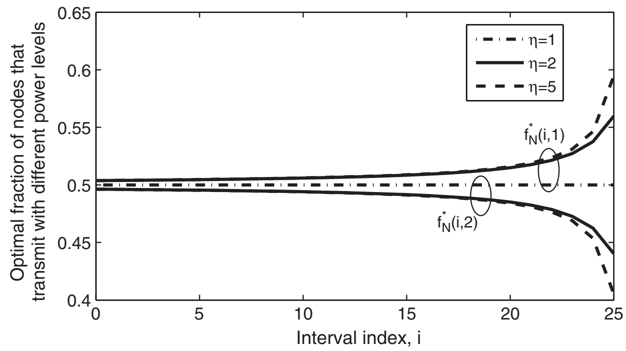

Fig. 6. Zoomed-in view of optimal fractions of nodes that transmit with different power levels for different η as a function of i ($N = 25$, $K = 10$, and $L = 2$).

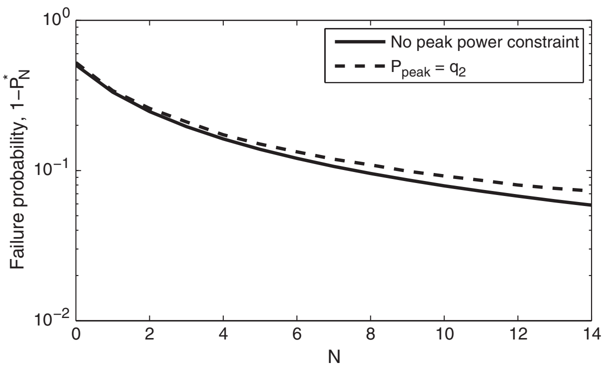

Fig. 7. Effect of peak power constraint: Zoomed-in view of failure probability: $1 - P^*_N$ as a function of N for different peak powers when the metric of a node is its channel power gain ($\eta = 1$, $K = 10$, and $L = 2$).

does not transmit if it cannot achieve the lowest target power q_1, as it cannot be decoded and selected.

Fig. 7 plots the failure probability of the proposed scheme as a function of N for $L = 2$ for $P_{\text{peak}} = q_2$ and ∞ (no peak power constraint). We see that even when P_{peak} is as small as q_2, the performance degradation is negligible. This is because the best node has the highest uplink channel power gain, which makes it unlikely that it will be affected by the constraint.

VI. Conclusion

We developed a new distributed node selection scheme in which a node jointly selects its timer value and its target receive power level based on its metric. The use of power control enables the best node to be selected even in the presence of simultaneous transmissions by other nodes with lower target powers. We first presented a general definition of an admissible metric-to-timer-and-power mapping, which ensured that the best node is selected in case of selection.

We then presented a recursive computation of the optimal mapping for two receive power levels with $\eta = 1$ and 2 and three target receive power levels with $\eta = 1$, which capture most of the gains from power control. We also saw that the recursions simplified considerably in the asymptotic regime of a large number of nodes, which manifested itself even when the number of nodes was as small as 10. We saw that the proposed scheme significantly outperformed the best known timer scheme in the literature. Future work involves analyzing the impact of imperfect power control on the proposed scheme.

Appendix

A. Proof of Result 1

Let $g : \mathcal{U} \to \mathcal{T} \times Q_L$ be any admissible mapping. Let us define another mapping $g_1 : \mathcal{U} \to \mathcal{T} \times Q_L$ as follows:

$$g_1(\mu) = \begin{cases} (0, \Xi_P(g(\mu))), & 0 \leq \Xi_T(g(\mu)) < \Delta_v, \\ g(\mu), & \Delta_v \leq \Xi_T(g(\mu)). \end{cases} \tag{30}$$

Thus, $g_1(.)$ affects only those nodes whose timers expire in $[0, \Delta_v)$. It makes all of them transmit at $t = 0$ and with the same target power as determined by the mapping $g(.)$. It can be verified that $g_1(.)$ is also an admissible mapping.

Now we show that the success probability using $g_1(.)$ is greater than or equal to that using $g(.)$. For any mapping, the success probability Pr(Success) can be written as

$$\begin{aligned} \Pr(\text{Success}) = &\Pr\left(\text{Success}|T_{[1]} \geq \Delta_v\right)\Pr\left(T_{[1]} \geq \Delta_v\right) \\ &+ \Pr\left(\text{Success}|T_{[1]} < \Delta_v, \Delta_v \leq T_{[2]}\right) \\ &\times \Pr\left(T_{[1]} < \Delta_v, \Delta_v \leq T_{[2]}\right) \\ &+ \Pr\left(\text{Success}|T_{[1]} < \Delta_v, T_{[2]} < \Delta_v\right) \\ &\times \Pr\left(T_{[1]} < \Delta_v, T_{[2]} < \Delta_v\right). \end{aligned} \tag{31}$$

The first term in the right hand side of (31) is the probability that none of the nodes transmit in $[0, \Delta_v)$ and a success occurs. It is the same for both $g(.)$ and $g_1(.)$. The second term is the probability that the timer of only node [1] expires in $[0, \Delta_v)$ and a success occurs. Here, $\Pr(T_{[1]} < \Delta_v, \Delta_v \leq T_{[2]})$ is the same for both $g(.)$ and $g_1(.)$. Given $T_{[1]} < \Delta_v$ and $T_{[2]} \geq \Delta_v$, from the construction of $g_1(.)$ in (30), $g_1(.)$ guarantees success, which may not be so in $g(.)$. Hence, in this case, the success probability of $g_1(.)$ is greater than or equal to that of $g(.)$.

The third term is the probability that the timers of nodes [1] and [2] expire in $[0, \Delta_v)$ and a success occurs. This happens due to power control and is not present in [8]. Here also, $\Pr(T_{[1]} < \Delta_v, T_{[2]} < \Delta_v)$ is the same for both $g(.)$ and $g_1(.)$. Given that $T_{[1]}$ and $T_{[2]}$ are in $[0, \Delta_v)$, the $\text{SINR}_{[1]}$ from $g_1(.)$ is greater than or equal to that from $g(.)$. Hence, in this case also, the success probability of $g_1(.)$ is greater than or equal to that of $g(.)$. Thus, the success probability of $g_1(.)$ is greater than or equal to that of $g(.)$. Repeated application of the above argument to timer values in $[\Delta_v, 2\Delta_v)$, $[2\Delta_v, 3\Delta_v)$, and so on leads to the desired result.

B. Proof of Result 3

We first prove $\alpha^*_N[0] > 0$ by showing that the success probability increases when $\alpha_N[0]$ increases from 0 to ε, where ε is infinitesimally small. Let $\alpha^*_N[0] = 0$, then, from (11), $P^*_N = P^*_{N-1}$. Now consider a new ILV $\widehat{\boldsymbol{\alpha}}_N$, in which $\widehat{\alpha}_N[0] = \varepsilon$

and $\widehat{\alpha}_N[i] = (1-\varepsilon)\alpha_N^*[i] = (1-\varepsilon)\alpha_{N-1}^*[i-1]$, for $1 \le i \le N$. Further, let $\widehat{\boldsymbol{F}}_N = \boldsymbol{F}_N^*$. The success probability of $[\widehat{\boldsymbol{\alpha}}_N, \widehat{\boldsymbol{F}}_N]$ is

$$P_N(\widehat{\boldsymbol{\alpha}}_N, \widehat{\boldsymbol{F}}_N) = \Pr(\mathcal{S}_0) + (1-\varepsilon)^K P_{N-1}^*. \tag{32}$$

From the law of total probability, we have

$$\Pr(\mathcal{S}_0) = \sum_{i=1}^{K} \Pr(\mathcal{S}_0, i \text{ nodes transmitted at } t=0). \tag{33}$$

The probability that i nodes transmit at $t=0$ is $\binom{K}{i}\varepsilon^i(1-\varepsilon)^{K-i}$. Hence, $\Pr(\mathcal{S}_0) = K\varepsilon + O(\varepsilon^2)$. Further, $(1-\varepsilon)^K P_{N-1}^* = (1 - K\varepsilon + O(\varepsilon^2))P_{N-1}^*$. Substituting these in (32), we get

$$P_N(\widehat{\boldsymbol{\alpha}}_N, \widehat{\boldsymbol{F}}_N) = P_{N-1}^* + K\varepsilon\left(1-P_{N-1}^*\right) + O(\varepsilon^2) > P_{N-1}^*, \tag{34}$$

where the strict inequality in (34) follows because $P_{N-1}^* < 1$, as the collision probability is strictly positive.

Next we prove that $\alpha_N^*[0] < 1$. For a given L, η, and K, let $\boldsymbol{\alpha}_N^* = \{1, 0, \ldots, 0\}$ and let the optimal PDM be $\boldsymbol{F}_N^*$. Let j_0 be the smallest non-zero integer such that $f_N^*(0, j_0) \neq 0$ and $f_N^*(0, j) = 0$, for $1 \le j < j_0$. It means that q_{j_0} is the smallest target receive power a node can have at $t = 0$. Consider a new ILV $\hat{\boldsymbol{\alpha}}_N = \{\hat{\alpha}_N[0], 1-\hat{\alpha}_N[0], \ldots, 0\}$, where $\hat{\alpha}_N[0] = 1 - f_N^*(0, j_0)/2$, and a new PDM $\hat{\boldsymbol{F}}_N$ in which $\hat{f}_N(0, j_0) = f_N^*(0, j_0)/(2\hat{\alpha}_N[0])$, $\hat{f}_N(0, j) = \hat{f}_N^*(0, j)/\hat{\alpha}_N[0]$, for $j_0 + 1 \le j \le L$, and $\hat{f}_N(0, j) = 0$, for $j < j_0$. Further, $\hat{f}_N(i, j) = 1$, for $i \ge 1$ and $j = 1$ and $\hat{f}_N(i, j) = 0$, for $i \ge 1$ and $j \neq 1$. Since $\sum_{j=1}^{L} \hat{f}_N(i, j) = 1$, for $0 \le i \le N$, $\hat{\boldsymbol{F}}_N$ is an admissible PDM. This choice of ILV and PDM ensures that the probability that a node has target receive power q_j, for $j_0 < j \le L$, at $t = 0$ is the same in both mappings. Hence, all the realizations of metrics that lead to a success for the mapping $[\boldsymbol{\alpha}_N^*, \boldsymbol{F}_N^*]$ will also lead to a success for $[\hat{\boldsymbol{\alpha}}_N, \hat{\boldsymbol{F}}_N]$.

Now consider a realization of metrics in which $\mu_{[1]} \in [f_N^*(0, j_0)/2, f_N^*(0, j_0))$ and $\mu_{[2]} < f_N^*(0, j_0)/2$. The probability of this realization is $K(f_N^*(0, j_0)/2)^K > 0$. In this realization, with the mapping $[\hat{\boldsymbol{\alpha}}_N, \hat{\boldsymbol{F}}_N]$, only node [1] transmits at $t=0$ with target receive power q_{j_0} and, thus, gets selected. However, with the mapping $[\boldsymbol{\alpha}_N^*, \boldsymbol{F}_N^*]$, all the K nodes transmit with target receive power q_{j_0} at $t = 0$ and collide. Thus, the success probability of $[\hat{\boldsymbol{\alpha}}_N, \hat{\boldsymbol{F}}_N]$ is strictly greater. Hence, $\alpha_N^*[0] \neq 1$.

The proof that $f_N^*(i, j) < 1$, for $0 \le i \le N$ and $1 \le j \le L$, is along similar lines, and is skipped to conserve space.

C. Proof of Result 4

Since $L = 2$, we have $f_N(i, 2) = 1 - f_N(i, 1)$, for $0 \le i \le N$. With optimal $\boldsymbol{\alpha}_N^*$ and $\boldsymbol{F}_N^*$, a success occurs at time $t = 0$ if: (i) Only node [1] transmits at $t = 0$. The probability of this event is $K\alpha_N^*[0](1-\alpha_N^*[0])^{K-1}$. Or, (ii) Node [1] has target power q_2 and node [2] has target power q_1 and only these two nodes transmit at $t = 0$. The probability of this event is $K(K-1)(\alpha_N^*[0])^2(1-\alpha_N^*[0])^{k-2}(1-f_N^*(0,1))f_N^*(0,1)$. Therefore, from (11), we get

$$\begin{aligned} P_N^* = &\ (1-\alpha_N^*[0])^K P_{N-1}^* + K\alpha_N^*[0]\,(1-\alpha_N^*[0])^{K-1} \\ &+ K(K-1)\,(\alpha_N^*[0])^2\,(1-\alpha_N^*[0])^{K-2} \\ &\times (1-f_N^*(0,1))\, f_N^*(0,1). \end{aligned} \tag{35}$$

Since $\boldsymbol{\alpha}_N^*$ and $\boldsymbol{F}_N^*$ are optimal, it can be seen from (35) that the function $\rho(x, y) = Kx(1-x)^{K-1} + K(K-1)x^2(1-x)^{K-2}(1-y)y + (1-x)^K P_{N-1}^*$ is maximized when $x = \alpha_N^*[0]$ and $y = f_N^*(0,1)$. From Result 3, we know that both $f_N^*(0,1)$ and $f_N^*(0,2)$ lie in $(0,1)$. Therefore, equating the derivative $\frac{\partial\rho(x,y)}{\partial y}$ to 0 gives $f_N^*(0,1) = 1/2$ and $f_N^*(0,2) = 1/2$. Along similar lines, we get $f_N^*(i,1) = f_N^*(i,2) = 1/2$, for $1 \le i \le N$. Substituting these results in (35) yields (12).

Further, equating $\frac{\partial\rho(x,\frac{1}{2})}{\partial x}|_{x=\alpha_N^*[0]}$ to 0, we find that $\alpha_N^*[0]$ is a root of the quadratic equation $ax^2 + bx - c = 0$, where $a = K^2 - 5K + 4P_{N-1}^*$, $b = 2K + 6 - 8P_{N-1}^*$, and $c = 4 - 4P_{N-1}^*$. When $K = 5$ and $N = 0$, this is a linear equation since $a = 0$. In this case, $\alpha_0^*[0] = c/b = 1/4$. Otherwise, the quadratic has two solutions $(x_2 \pm \sqrt{x_1})/x_3$, where $x_1 = (5K-9)(K-1) - P_{N-1}^*(4K-8)(K-1)$, $x_2 = K + 3 - 4P_{N-1}^*$, and $x_3 = K(5-K) - 4P_{N-1}^*$. However, $(x_2 + \sqrt{x_1})/x_3$ cannot be $\alpha_N^*[0]$ for any K. This is because for $K = 2$, we get $(x_2 + \sqrt{x_1})/x_3 = 1$, which is suboptimal from Result 3; for $K = 3$ and 4, $(x_2 + \sqrt{x_1})/x_3 > 1$; and, for $K \ge 5$, $(x_2 + \sqrt{x_1})/x_3 < 0$.

D. Proof of Result 5

First, we prove that the choice of $\check{\boldsymbol{\alpha}}_N^*$ and $\check{\boldsymbol{F}}_N^*$ in (19), (20), and (21) yields a lower bound on the success probability. Thereafter, we explain the intuition behind the recursion.

Formal Proof: Since $\check{f}_N^*(i,1) = \check{f}_N^*(i,2) = 1/2$, for $0 \le i \le N$, the PDM is clearly admissible. We next prove using induction over N that the recursion in (19) and (20) also leads to an ILV that is admissible. For this, we need to prove that $\check{\alpha}_N^*[i] \ge 0$, for $0 \le i \le N$, and $\sum_{i=0}^{N} \check{\alpha}_N^*[i] \le 1$.

We observe that $\check{\alpha}_0^*[0]$, which is given in (19), equals $\alpha_0^*[0]$, which is given in (13), because $P_{-1}^* = \check{P}_{-1}^* = 0$. Hence, from the proof in the last part of Appendix C, it follows that $0 < \check{\alpha}_0^*[0] < 1$. Thus, the ILV $\check{\boldsymbol{\alpha}}_0^* = (\check{\alpha}_0[0])$ is admissible. Further, $\check{P}_0^*$, which is given in (18), lies in (0,1). This is because $\check{P}_0^* < \sum_{i=0}^{K}\binom{K}{i}(\check{\alpha}_N^*[0])^i(1-\check{\alpha}_N^*[0])^{K-i} = 1$, and from (18) it is obvious that $\check{P}_0^* > 0$.

Let us assume that the ILV $\check{\boldsymbol{\alpha}}_N^*$ is admissible and $\check{P}_N^* \in (0,1)$ for $N = M$. The expression for $\alpha_{M+1}^*[0]$ in (13) is the same as that for $\check{\alpha}_{M+1}^*[0]$ in (19) except that P_M^* is replaced with $\check{P}_M^*$, both of which lie in (0,1). From Appendix C, it follows that $0 < \check{\alpha}_{M+1}^*[0] < 1$. Further, from the admissibility of $\check{\boldsymbol{\alpha}}_N^*$ and (20), it follows that $0 \le \check{\alpha}_{M+1}^*[i] \le 1$, for $1 \le i \le M+1$. Now, $\sum_{i=0}^{M+1} \check{\alpha}_{M+1}^*[i] = \check{\alpha}_{M+1}^*[0] + (1-\check{\alpha}_{M+1}^*[0])\sum_{i=0}^{M} \check{\alpha}_M^*[i]$. Since $\sum_{i=0}^{M} \check{\alpha}_M^*[i] \le 1$, we get $\sum_{i=0}^{M+1} \check{\alpha}_{M+1}^*[i] \le 1$. Further, it can be shown that $\check{P}_{M+1}^* \in (0,1)$ because $\check{\alpha}_{M+1}^*[0]$ and $\check{P}_M^*$ lie in $(0,1)$. Thus, we see that $\check{\boldsymbol{\alpha}}_N^*$ is also admissible.

Intuition Behind Recursion: For $L = 2$ with $\eta = 2$, a success occurs at time $t = 0$ for the mapping $[\boldsymbol{\alpha}_N, \boldsymbol{F}_N]$ if:

1) Only node [1] transmits at $t = 0$. This happens with probability $K\alpha_N[0](1-\alpha_N[0])^{K-1}$.
2) Or, only nodes [1] and [2] transmit at $t = 0$ with target powers q_2 and q_1, respectively. The probability of this event is $K(K-1)(\alpha_N[0])^2(1-\alpha_N[0])^{k-2}(1-f_N(0,1))f_N(0,1)$.

3) Or, only nodes [1], [2], and [3] transmit at $t=0$ with target powers q_2, q_1, and q_1, respectively. The probability of this event is $\binom{K}{2,1}(\alpha_N[0])^3(1-\alpha_N[0])^{K-3}(1-f_N(0,1))(f_N(0,1))^2$.

Hence, the success probability $P_N(\boldsymbol{\alpha}_N,\boldsymbol{F}_N)$ is given by

$$\begin{aligned}P_N(\boldsymbol{\alpha}_N,\boldsymbol{F}_N) = {} & (1-\alpha_N[0])^K P_{N-1}\left(\boldsymbol{\alpha}'_{N-1},\boldsymbol{F}'_{N-1}\right)\\ &+ K\alpha_N[0](1-\alpha_N[0])^{K-1}\\ &+ K(K-1)(\alpha_N[0])^2(1-\alpha_N[0])^{K-2}\\ &\times (1-f_N(0,1))f_N(0,1)\\ &+\binom{K}{2,1}(\alpha_N[0])^3(1-\alpha_N[0])^{K-3}\\ &\times (1-f_N(0,1))(f_N(0,1))^2, \end{aligned} \tag{36}$$

where $\boldsymbol{\alpha}'_{N-1}$ and $\boldsymbol{F}'_{N-1}$ are defined in (6) and (7). Neglecting the event in which three nodes transmit, we get $P_N(\boldsymbol{\alpha}_N,\boldsymbol{F}_N)\geq(1-\alpha_N[0])^K P_{N-1}(\boldsymbol{\alpha}'_{N-1},\boldsymbol{F}'_{N-1})+K\alpha_N[0](1-\alpha_N[0])^{K-1}+K(K-1)(\alpha_N[0])^2(1-\alpha_N[0])^{K-2}(1-f_N(0,1))f_N(0,1)$.

Motivated by this bound and the recursion in (9), we propose the following recursion to determine $\check{\alpha}_N^*[0]$ and $\check{f}_N^*(0,1)$. The remaining elements of $\check{\boldsymbol{\alpha}}_N^*$ and $\check{\boldsymbol{F}}_N^*$ are then determined as $\check{\alpha}_N^*[i]=\check{\alpha}_{N-1}^*[i-1](1-\check{\alpha}_N^*[0])$ and $\check{f}_N^*(i,1)=\check{f}_{N-1}^*(i-1,1)$, respectively, for $i=1,\ldots,N$. Let $H(x,y;z)=(1-x)^K z+Kx(1-x)^{K-1}+K(K-1)x^2(1-x)^{K-2}(1-y)y$, where $z\in[0,1)$. Note that $H(x,y;P_{N-1}^*)=\rho(x,y)$, which is defined below (35). It can be shown that the optimal $x\in[0,1]$ that maximizes $H(x,y;z)$ is equal to $\alpha_N^*[0]$, which is given by (13) with P_{N-1}^* replaced by z. Furthermore, the optimal $y\in[0,1]$ is 1/2. We use this in all the steps below.

For $N=0$, $[\check{\alpha}_0^*[0],\check{f}_0^*(0,1)]=\arg\max_{x,y \atop x,y\in[0,1]} H(x,y;0)$. Let $\check{P}_0^*$ denote the success probability calculated using the formula in (36) with $N=0$, ILV $\check{\boldsymbol{\alpha}}_0^*$, and PDM $\check{\boldsymbol{F}}_0^*$. Then, for $N=1$, $[\check{\alpha}_1^*[0],\check{f}_1^*(0,1)]=\arg\max_{x,y \atop x,y\in[0,1]} H(x,y;\check{P}_0^*)$. Let $\check{P}_1^*$ denote the success probability calculated using (36) with $N=1$, ILV $\check{\boldsymbol{\alpha}}_1^*$, and PDM $\check{\boldsymbol{F}}_1^*$. In general, let $\check{P}_{N-1}^*$ denote the success probability calculated using (36) using ILV $\check{\boldsymbol{\alpha}}_{N-1}^*$ and PDM $\check{\boldsymbol{F}}_{N-1}^*$ in the $(N-1)^{\text{th}}$ step. Then, in the N^{th} step, $[\check{\alpha}_N^*[0],\check{f}_N^*(0,1)]=\arg\max_{x,y \atop x,y\in[0,1]} H(x,y;\check{P}_{N-1}^*)$. Thus, the recursion in Result 5 follows.

E. Proof of Result 6

With $\boldsymbol{\alpha}_N$ and $\boldsymbol{F}_N$, a success occurs at $t=0$ if one of the following mutually exclusive events occurs at $t=0$: only node [1] transmits. This happens with probability $K\alpha_N[0](1-\alpha_N[0])^{K-1}$. Or, only nodes [1] and [2] transmit. Node [1] transmits with target power q_3 and node [2] transmits with target power q_1 or q_2. This happens with probability $\binom{K}{1,1}(\alpha_N[0])^2(1-\alpha_N[0])^{K-2}f_N(0,3)(f_N(0,1)+f_N(0,2))$. Or, nodes [1] and [2] transmit with target powers q_2 and q_1, respectively, and no other node transmits. This happens with probability $\binom{K}{1,1}(\alpha_N[0])^2(1-\alpha_N[0])^{K-2}f_N(0,2)f_N(0,1)$. Or, node [1] transmits with target power q_3 and m other nodes transmit with target power q_1, where $2\leq m\leq\min\{K-1,\psi\}$, where $\psi=\lfloor\eta\gamma(\eta+\sigma^2/q_1)\rfloor$. This happens with probability $\binom{K}{m,1}(\alpha_N[0])^{m+1}(1-\alpha_N[0])^{K-m-1}f_N(0,3)(f_N(0,1))^m$. Therefore, the success probability is given by

$$\begin{aligned}P_N(\boldsymbol{\alpha}_N,\boldsymbol{F}_N) = {} & (1-\alpha_N[0])^K P_{N-1}\left(\boldsymbol{\alpha}'_{N-1},\boldsymbol{F}'_{N-1}\right)\\ &+ K\alpha_N[0](1-\alpha_N[0])^{K-1}\\ &+ K(K-1)(\alpha_N[0])^2(1-\alpha_N[0])^{K-2}\\ &\times (f_N(0,3)(f_N(0,2)+f_N(0,1))\\ &+ f_N(0,2)f_N(0,1))\\ &+\sum_{m=2}^{\min\{K-1,\psi\}}\binom{K}{m,1}(1-\alpha_N[0])^{K-m-1}\\ &\times (\alpha_N[0])^{m+1}f_N(0,3)(f_N(0,1))^m. \end{aligned} \tag{37}$$

Consider, instead, the following recursion that is obtained by neglecting the fourth event above:

$$\begin{aligned}\widetilde{P}_N(\boldsymbol{\alpha}_N,\boldsymbol{F}_N) = {} & (1-\alpha_N[0])^K \widetilde{P}_{N-1}\left(\boldsymbol{\alpha}'_{N-1},\boldsymbol{F}'_{N-1}\right)\\ &+ K\alpha_N[0](1-\alpha_N[0])^{K-1}\\ &+ K(K-1)(\alpha_N[0])^2(1-\alpha_N[0])^{K-2}\\ &\times (f_N(0,3)(1-f_N(0,3))\\ &+ f_N(0,2)f_N(0,1)), \end{aligned} \tag{38}$$

where $\widetilde{P}_{-1}(\boldsymbol{\alpha}'_{-1},\boldsymbol{F}'_{-1})=0$ for all $\boldsymbol{\alpha}'_{-1}$ and $\boldsymbol{F}'_{-1}$. By induction, one can show that $P_N^*\geq P_N(\boldsymbol{\alpha}_N,\boldsymbol{F}_N)\geq\widetilde{P}_N(\boldsymbol{\alpha}_N,\boldsymbol{F}_N)$, for all $N\geq 0$, thus, giving a lower bound of P_N^*.

We now maximize $\widetilde{P}_N(\boldsymbol{\alpha}_N,\boldsymbol{F}_N)$ to tighten the lower bound. Let $\widetilde{P}_N^*$ be the maximum value of $\widetilde{P}_N(\boldsymbol{\alpha}_N,\boldsymbol{F}_N)$, which is achieved with ILV $\widetilde{\boldsymbol{\alpha}}_N^*$ and PDM $\widetilde{\boldsymbol{F}}_N^*$. Then, it can be shown that

$$\begin{aligned}\widetilde{P}_N^* = {} & (1-\widetilde{\alpha}_N^*[0])^K\widetilde{P}_{N-1}^*+K\widetilde{\alpha}_N^*[0](1-\widetilde{\alpha}_N^*[0])^{K-1}\\ &+ K(K-1)(\widetilde{\alpha}_N^*[0])^2(1-\widetilde{\alpha}_N^*[0])^{K-2}\\ &\times\left(\widetilde{f}_N^*(0,3)\left(1-\widetilde{f}_N^*(0,3)\right)+\widetilde{f}_N^*(0,1)\widetilde{f}_N^*(0,2)\right), \end{aligned} \tag{39}$$

which is obtained by setting $\widetilde{\alpha}_N^*[i+1]=\widetilde{\alpha}_{N-1}^*[i](1-\widetilde{\alpha}_N^*[0])$, for $0\leq i\leq N-1$, and $\widetilde{f}_N^*(i+1,j)=\widetilde{f}_{N-1}^*(i,j)$, for $0\leq i\leq N-1$ and $1\leq j\leq L$.

Since $\widetilde{\boldsymbol{\alpha}}_N^*$ and $\widetilde{\boldsymbol{F}}_N^*$ achieve $\widetilde{P}_N^*$, it can be seen from (39) that the function $Q(x,y_1,y_2)=Kx(1-x)^{K-1}+K(K-1)x^2(1-x)^{K-2}(y_1(1-y_1)+(1-y_1-y_2)y_2)+(1-x)^K\widetilde{P}_{N-1}^*$ attains its maximum value when $x=\widetilde{\alpha}_N^*[0]$, $y_1=\widetilde{f}_N^*(0,3)$, and $y_2=\widetilde{f}_N^*(0,1)$. As in Appendix B, we can show that $\widetilde{f}_N^*(0,1)=\widetilde{f}_N^*(0,2)=\widetilde{f}_N^*(0,3)=1/3$. Substituting these values in (39) results in (24).

Further, equating $\partial Q(x,1/3,1/3)/\partial x$ to zero, we get $\widetilde{\alpha}_N^*[0]$ as the solution of the following quadratic equation: $\widetilde{a}x^2+\widetilde{b}x+\widetilde{c}=0$, where $\widetilde{a}=K^2-4K+3\widetilde{P}_{N-1}^*$, $\widetilde{b}=K+5-6\widetilde{P}_{N-1}^*$, and $\widetilde{c}=-3(1-\widetilde{P}_{N-1}^*)$. For $K=4$ and $N=0$, it is a linear equation with root $\widetilde{\alpha}_0^*[0] = 1/3$. Otherwise, it has two solutions $(-\widetilde{b} \pm \sqrt{\widetilde{b}^2 - 4\widetilde{a}\widetilde{c}})/(2\widetilde{a})$. It can again be shown that $\widetilde{\alpha}_N^*[0] \neq (-\widetilde{b} - \sqrt{\widetilde{b}^2 - 4\widetilde{a}\widetilde{c}})/(2\widetilde{a})$.

REFERENCES

[1] A. Bletsas, A. Khisti, D. P. Reed, and A. Lippman, "A simple cooperative diversity method based on network path selection," *IEEE J. Sel. Areas Commun.*, vol. 24, no. 3, pp. 659–672, Mar. 2006.

[2] Y. Jing and H. Jafarkhani, "Single and multiple relay selection schemes and their achievable diversity orders," *IEEE Trans. Wireless Commun.*, vol. 8, no. 3, pp. 1414–1423, Mar. 2009.

[3] D. Tse and P. Vishwanath, *Fundamentals of Wireless Communications*. Cambridge, U.K.: Cambridge Univ. Press, 2005.

[4] Y. Chen and Q. Zhao, "An integrated approach to energy-aware medium access for wireless sensor networks," *IEEE Trans. Signal Process.*, vol. 55, no. 7, pp. 3429–3444, Jul. 2007.

[5] D. S. Michalopoulos and G. K. Karagiannidis, "PHY-layer fairness in amplify and forward cooperative diversity systems," *IEEE Trans. Wireless Commun.*, vol. 7, no. 3, pp. 1073–1082, Mar. 2008.

[6] X. Qin and R. Berry, "Opportunistic splitting algorithms for wireless networks," in *Proc. INFOCOM*, Mar. 2004, pp. 1662–1672.

[7] V. Shah, N. B. Mehta, and R. Yim, "Splitting algorithms for fast relay selection: Generalizations, analysis, a unified view," *IEEE Trans. Wireless Commun.*, vol. 9, no. 4, pp. 1525–1535, Apr. 2010.

[8] V. Shah, N. B. Mehta, and R. Yim, "Optimal timer based selection schemes," *IEEE Trans. Commun.*, vol. 58, no. 6, pp. 1814–1823, Jun. 2010.

[9] H. Wang, S. Yang, and J. Lin, "A distributed selection cooperation protocol with feedback and its DMT in Nakagami-m fading channels," *IEEE Commun. Lett.*, vol. 13, no. 11, pp. 844–846, Nov. 2009.

[10] Q. Zhao and L. Tong, "Opportunistic carrier sensing for energy-efficient information retrieval in sensor networks," *EURASIP J. Wireless Commun. Netw.*, vol. 2, pp. 231–241, Apr. 2005.

[11] R. Talak and N. B. Mehta, "Optimal timer-based best node selection for wireless systems with unknown number of nodes," *IEEE Trans. Commun.*, vol. 61, no. 11, pp. 4475–4485, Nov. 2013.

[12] Y. Xiao and L. J. Cimini, "Impact of overhead on spectral efficiency of cooperative relaying," *IEEE Trans. Wireless Commun.*, vol. 12, no. 5, pp. 2228–2239, May 2013.

[13] A. Zanella and M. Zorzi, "Theoretical analysis of the capture probability in wireless systems with multiple packet reception capabilities," *IEEE Trans. Commun.*, vol. 60, no. 4, pp. 1058–1071, Apr. 2012.

[14] G. D. Nguyen, A. Ephremides, and J. E. Wieselthier, "On capture in random-access systems," in *Proc. ISIT*, Jul. 2006, pp. 2072–2076.

[15] R. Yim, N. B. Mehta, and A. F. Molisch, "Fast multiple access selection through variable power transmissions," *IEEE Trans. Wireless Commun.*, vol. 8, no. 4, pp. 1962–1973, Apr. 2009.

[16] R. O. LaMaire, A. Krishna, and M. Zorzi, "On the randomization of transmitter power levels to increase throughput in multiple access radio systems," *Wireless Netw.*, vol. 4, no. 3, pp. 263–277, Mar. 1998.

[17] A. D. Gore and A. Karandikar, "Power-controlled FCFS splitting algorithm for wireless networks," *IEEE Trans. Veh. Technol.*, vol. 59, no. 2, pp. 842–856, Feb. 2010.

[18] V. K. Dewangan and N. B. Mehta, "Capture-induced, fast, distributed, splitting based selection with imperfect power control," *IEEE Trans. Commun.*, vol. 62, no. 1, pp. 74–84, Jan. 2014.

[19] K. Cohen and A. Leshem, "Energy-efficient detection in wireless sensor networks using likelihood ratio and channel state information," *IEEE J. Sel. Areas Commun.*, vol. 29, no. 8, pp. 1671–1683, Sep. 2011.

[20] L. Fan, X. Lei, R. Q. Hu, and W. Seah, "Outdated relay selection in two-way relay network," *IEEE Trans. Veh. Technol.*, vol. 62, no. 8, pp. 4051–4057, Oct. 2013.

[21] S. N. Datta, S. Chakrabarti, and R. Roy, "Performance analysis of distributed selection combining with dual-hop relay link in Rayleigh fading channel," in *Proc. ICCS*, Nov. 2010, pp. 361–365.

[22] K. J. Ray Liu, A. K. Sadek, W. Su, and A. Kwasinski, *Cooperative Communications and Networking*. Cambridge, U.K.: Cambridge Univ. Press, 2009.

[23] X. Qin and R. Berry, "Exploiting multiuser diversity for medium access control in wireless networks," in *Proc. INFOCOM*, Apr. 2003, pp. 1084–1094.

[24] T. Tang and R. W. Heath, "Opportunistic feedback for downlink multiuser diversity," *IEEE Commun. Lett.*, vol. 9, no. 10, pp. 948–950, Oct. 2005.

[25] A. Papoulis and S. U. Pillai, *Probability, Random Variables and Stochastic Processes*., 4th ed. New York, NY, USA: McGraw-Hill, 2002.

[26] A. J. Izenman, "Recent developments in nonparametric density estimation," *J. Am. Statist. Assoc.*, vol. 86, no. 413, pp. 205–224, Mar. 1991.

[27] J. Lee *et al.*, "An experimental study on the capture effect in 802.11a networks," in *Proc. WinTECH*, Sep. 2007, pp. 19–26.

Vikas Kumar Dewangan received the B.Eng. degree in electronics and communication engineering from Maulana Azad College of Technology, Bhopal, India, in 1998 and the M.Tech. degree in communication and radar engineering from the Indian Institute of Technology, New Delhi, India, in 1999. He is currently working toward the Ph.D. degree with the Department of Electrical Communication Engineering, Indian Institute of Science, Bangalore, India. He is also currently a Scientist of the Defence Research and Development Organization (DRDO), India. His research interests include multiple access protocols, radar data and signal processing, and target identification.

Neelesh B. Mehta (S'98–M'01–SM'06) received the B.Tech. degree in electronics and communications engineering from the Indian Institute of Technology (IIT), Madras, Chennai, India, in 1996 and the M.S. and Ph.D. degrees in electrical engineering from the California Institute of Technology, Pasadena, CA, USA, in 1997 and 2001, respectively. He is currently an Associate Professor with the Department of Electrical Communication Engineering, Indian Institute of Science (IISc), Bangalore, India. He currently serves as a Member-at-Large on the Board of Governors of the IEEE Communication Society. He serves as an Executive Editor of the IEEE TRANSACTIONS ON WIRELESS COMMUNICATION and as an Editor of the IEEE TRANSACTIONS ON COMMUNICATIONS and IEEE WIRELESS COMMUNICATION LETTERS.